Hydrodynamic Fluctuations in Liquids Observed by NMR-Modulated Gradient Spin-Echo Method

Janez Stepišnik

Applied Magnetic Resonance

ISSN 0937-9347

Appl Magn Reson
DOI 10.1007/s00723-020-01253-7

Springer

Applied Magnetic Resonance
https://doi.org/10.1007/s00723-020-01253-7

Applied
Magnetic Resonance

ORIGINAL PAPER

Hydrodynamic Fluctuations in Liquids Observed by NMR-Modulated Gradient Spin-Echo Method

Janez Stepišnik[1]

Received: 16 May 2020 / Revised: 4 August 2020

Abstract

The modulated gradient spin echo is an NMR method that provides direct insight into the low-frequency part of the molecular velocity auto-correlation spectra in fluids. Because the method gives a spectrum that is time-averaged over the trajectory elapsed, the spins are able to observe local inhomogeneities in the initial interval after spin excitation. In fluid measurements, it manifests as an initial non-exponential decay of the spin-echo signals, which we attribute to the spatial heterogeneity of molecular self-diffusion due to the molecular motion in microvortices of hydrodynamic oscillations. The hydrodynamic fluctuations occur in water, ethanol, toluene, and a mixture of water with lower glycerol content, while they disappeared with increasing glycerol content.

1 Introduction

One of the significant discoveries in the field of molecular dynamic in fluids is the existence of hydrodynamic fluctuations [11, 13, 14, 30] that results in a non-exponential long-time tail of the molecular velocity auto-correlation function (VAF), with the power law decay $\approx t^{-3/2}$ for 3D systems. The hydrodynamic fluctuation phenomena were first predicted on the ground of Landau–Lifshitz theory, but the discovery gained momentum after the confirmation of phenomena by the simulations of hard-sphere fluid dynamics [2], which shows that a diffusing hard spheres develop a vortex backflow effect responsible for the persistence of the VAF at long times [3]. The hydrodynamic fluctuations cause the dispersion of the viscosity coefficient or thermal conductivity [14], and can also affect the molecular self-diffusion in liquids [26, 27]. Studies of hydrodynamic fluctuations in non-equilibrium systems are known, where their intensities can cover the whole system and which are strongly influenced by gravity and

✉ Janez Stepišnik
janez.stepisnik@fmf.uni-lj.si

[1] Faculty of Mathematics and Physics, University of Ljubljana, Jadranska 19, 1000 Ljubljana, Slovenia

Published online: 28 August 2020

confinement [6]. However, we deal here with hydrodynamic fluctuations in fluids that are in thermodynamic equilibrium.

The VAF is a key quantity of the molecular translation dynamics containing information about the underlying processes of molecular interaction in fluids, but its measurement by neutron [4, 15, 20] and light scattering [17] method does not provide very conclusive results on the asymptotic long-time behavior of VAF due to the short-time scale limits of methods [5]. Thus, the measurement of the VAF asymptotic behavior in dense systems remains a challenge, which complete understanding cannot be revealed by using the traditional experimental techniques. Scientific efforts are, therefore, focused on finding methods that are not related to these main research tools to be able to dig deeply in the details of the hydrodynamic fluctuation phenomena. For this purpose, the method of the molecular self-diffusion measurements was used, among which the measurement by NMR gradient spin-echo method gained the main utility. Most widely used is the measurement of self-diffusion coefficient, D, by method of two pulsed gradient spin-echo (PGSE) [10], but a greater potential applicability has the method of modulated gradient spin-echo (MGSE) [7, 8, 21] which allows direct measurements not only of D but also of the low-frequency part of the power spectrum of VAF, i.e., the velocity auto-correlation spectrum (VAS). Experiments have shown that the measurement of VAS by the MGSE method allows the discovery of new details about the molecular dynamics in the polymer melts [28], in fluidized granular motion [16], in restricted diffusion in porous systems [9, 19, 24, 25, 29], and in transverse molecular motion in liquids [26, 27].

2 Modulated Gradient Spin-Echo Method

In liquids, rapid molecular motion on the time scale of picoseconds or nanoseconds completely nullifies the spin dipole–dipole and the first-order quadrupole interactions, while the spin interactions with electrons in molecular orbitals and the electron mediated spin–spin interactions cannot be ignored. They appear as the chemical shifts and J couplings in the NMR spectrum. Fluctuation of these interactions can be characterized by correlation functions of relevant physical quantities and affect spin relaxation. However, in the case of the use of NMR gradient spin-echo methods, the applied MFG is usually strong enough that the effect of fluctuation of molecular translation velocity dominates in echo attenuation over all other interactions. It allows to approximate the decay of the spin-echo peak signals at the time τ, by:

$$E(\tau) = \sum_i E_{oi} e^{i\alpha_i(\tau) - \beta_i(\tau)}, \tag{1}$$

where the sum goes over the sub-ensembles of spins with identical dynamical properties. The phase shift

$$\alpha_i(\tau) = \int_0^\tau \mathbf{q}(t) \cdot \langle \mathbf{v}_i(t) \rangle \mathrm{d}t \tag{2}$$

can be neglected, when the averaged velocity of spin bearing particle is zero, $\langle \mathbf{v}_i(t) \rangle = 0$. This is not in the case of collective molecular motion or diffusion in non-homogeneous systems like porous media [23], while the spin-echo attenuation can be expressed as:

$$\beta_i(\tau) = \frac{1}{\pi} \int_0^\infty \mathbf{q}(\omega, \tau) \mathbf{D}_i(\omega, \tau) \mathbf{q}^*(\omega, \tau) \, \mathrm{d}\omega. \tag{3}$$

Here, $\mathbf{q}(\omega, \tau)$ is the spectrum of the spin phase discord $\mathbf{q}(t)$ created by the radiofrequency (RF) pulses and MFG [26], and where:

$$\mathbf{D}_i(\omega, \tau) = \int_0^\infty \langle \mathbf{v}_i(t) \otimes \mathbf{v}_i(0) \rangle_\tau \cos(\omega t) \mathrm{d}t \tag{4}$$

is the VAS. The application of PGSE method for the study of VAS in liquids is limited by the induction of gradient coil, which prevents the formation of short enough interval between two MFG pulses. However, the MGSE method, which directly probes the low-frequency part of VAS, is more adequate method for the study of the long-time asymptotic properties of VAF in the dense systems. It extracts the data about the VAS by the "stroboscopic" modulation of the spatial dispersion of the spin phase using an appropriate sequence of RF pulses and MFG pulses or waveform. It is basically a Carr–Purcell–Meiboom–Gill sequence (CPMG) consisting of initial $\pi/2$-RF pulse and the train of N π-RF pulses separated by time intervals T [10, 18] applied in the background of MFG. The first applications of MGSE method with pulsed or oscillating MFG demonstrated among others also how the MGSE sequence improves the resolution of the diffusion-weighted MR images of the brain and the MRI of the diffusion tensor of neurons [1]. In the case of PGSE, the frequency range of MGSE with the pulsed MFG is limited to below 1 kHz due to the gradient coil self-inductance. With the development of the MGSE technique in fixed MFG [21, 22], the gradient coil induction limit was avoided, and a much higher frequency limit is determined by the power of the RF transmitter and the magnitude of the MFG, while the lowest limit remains inversely proportional to the spin relaxation time. The use of the MGSE techniques with fixed MFG was first proposed in reference [8] with concern about the side effects of using RF pulses in the presence of background MFG. The analysis of adverse interference of both fields [24, 26] shows that at suitable experimental conditions, the MGSE signal decay can be described as:

$$E(\tau, \omega_m) = \sum_i E_{oi} e^{-\frac{\tau}{T_{2i}} - \frac{4\gamma^2 G^2}{\pi^2 \omega_m^2} D_{zzi}(\omega_m, \tau)\tau}, \tag{5}$$

where T_{2i} is the spin relaxation, $\tau = NT$, and $D_{zzi}(\omega_m, \tau)$ is a component of the VAS tensor at the modulation frequency $\omega_m = \pi/T$, which is determined by the direction of applied MFG. Index τ in $D_{zzi}(\omega_m, \tau)$ means that the time averaging over the particle trajectory elapsed in the interval τ. The advantage of the new MGSE technique was demonstrated by measuring the VAS of restricted diffusion in pores

smaller than 0.1 μm [24], by measuring the VAS of granular dynamics in fluidized granular systems [16] and by the discovery of a new low-frequency mode of motion in polymer melts [28]. Instead of using the externally applied MFG, this technique allows the exploitation of the static MFG generated by the susceptibility differences on interfaces inside porous systems to obtain information about the pore morphology and distribution of internal MFG [24].

Since $D_{zzi}(\omega_m, \tau)$ is the time-averaged spectrum from the moment of spin excitation to the signal detection at time τ, the signals induced by spins at different sites in the media can, in the initial short intervals of measurement, convey information about local inhomogeneities, which may result either from the distribution of the internal MFG like in the porous medium [24] or from the diversity of motion due to fluxes or hydrodynamic fluctuations in liquids as in our case [26, 27]. By grouping the spin bearing particles into separate sub-ensembles corresponding to spins with the different attenuation coefficient, the induction signal can be described by the distribution function $P(D)$ as $E(\tau) = \int P(D)e^{-sD\tau}\mathrm{d}D$ with $s = \frac{4\gamma^2G^2}{\pi^2\omega^2}$ as given in Eq. (5). In the case of narrow distribution, the signal attenuation can be expanded as:

$$\beta(\tau) \approx \tau/T_2 + s\langle D\rangle\tau - \frac{s^2}{2}\langle \Delta D^2\rangle\tau^2 + \ldots, \tag{6}$$

where $\langle D\rangle$ is the mean diffusion coefficient and $\langle \Delta D^2\rangle$ is the variance of the distribution. It gives a non-exponential decay of the echos, and the time derivative of $\beta(\tau)$ gives an apparent diffusion coefficient, $D_{\mathrm{app}}(\omega, \tau)$, containing data on the mean self-diffusion coefficient and its distribution.

3 Experiments

NMR spectrometer with 100 MHz proton Larmor frequency equipped with the Maxwell gradient coils to generate MFG in steps to the maximum of 5.7 T/m was used to measure the VAS of three polar liquids: distillate water, ethanol (analytical standard-Sigma-Aldrich), and glycerol (99.5% Sigma-Aldrich) with the dipole moments of 1.85D, 1.69D, and 2.56D respectively, non-polar toluene (99.8% Sigma-Aldrich), and the mixtures of glycerol (99.5% Sigma-Aldrich) and water at room temperatures. Samples of glycerol/water mixtures were kept in plastic bottles of 100 ml volume for several days before used for the measurements. The samples were loaded into 15 mm-long and 5 mm-wide pyrex glass ampules and closed with paraffin tape to be inserted in the head of the 100 MHz NMR spectrometer. To avoid a possible impact of restricted diffusion, containers with the diameter much larger than the molecular displacements in the time of 100 ms long-time intervals of measurement were used. In addition, the effect of restricted diffusion is even further reduced by the initial $\pi/2$-RF pulse of the MGSE sequence applied in the background of MFG, because it excites only a few mm narrow slice of sample.

4 Results and Discussion

Data of the MGSE measurements of liquids were analyzed in the following way. The τ-dependencies of spin-echo signal peaks taken at various T were fitted by a fifth-order polynomial series. The time derivative of these fits represents the apparent diffusion spectrum (ADS) if the attenuation caused by the spin relaxation is deducted in this calculation. The dependencies of the ADS on τ thus calculated show deviations from the expected monoexponential decay of the spin-echo amplitudes, which occurs of all samples of liquids and mixtures considered, but not in G/W mixtures with high glycerol contents. Figure 1 shows the 3D frequency-temporal plot of ADS for water, obtained from the time derivatives of $\beta(\tau)$ curves obtained by fitting to the echo peaks with the coefficient of determination $R^2 > 0.99999$. On its surface in the area of short times and high frequencies is clearly visible hump due to deviations from the monoexponential decay. We interpreted curved surface by the molecular diffusion diversity due to the motion in the vortexes of hydrodynamic fluctuations [26, 27]. The part of curved surface is more clearly visible in the contour plot of the second derivative of $\beta(\tau)$, which is proportional to the variance of VAS distribution, $\langle \Delta D^2 \rangle$, as shown in Figs. 2, 3 and 4 for water, ethanol, and toluene, respectively, and in Figs. 5 and 6 for the G/W mixtures. In all cases, $\langle \Delta D^2 \rangle$ occurs at higher modulation frequencies and disappears at longer time intervals, $\tau > 40$ ms, when the spin trajectories are long enough to span the whole extend of heterogeneity and to average off the diffusion diversity, $\langle \Delta D^2 \rangle = 0$. Figures 4 and 5 show how the effect of fluctuation on $\langle \Delta D^2 \rangle$ decreases with the increase of glycerol content from 5 to 15 vol% and then disappears at concentrations higher than 30 vol% [27].

Table 1 shows the correlation times, τ_c, and magnitudes, Δz, of the vortexes of hydrodynamic fluctuations, as they can be roughly estimated from the images of $\langle \Delta D^2 \rangle$ in Figs. 3, 4, 5, and 6 with the relative error of about 30%.

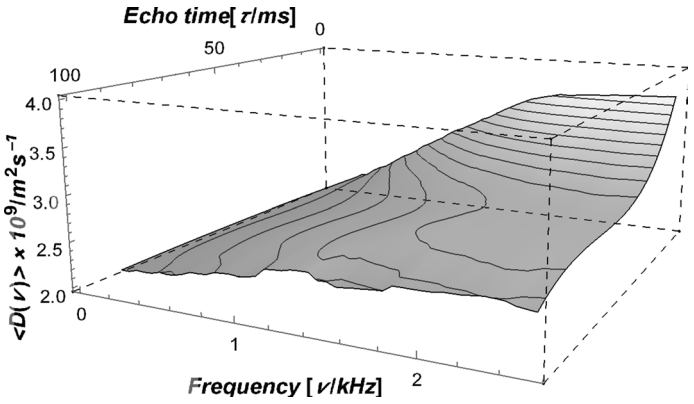

Fig. 1 3D temporal-frequency plot of the apparent self-diffusion coefficient of water

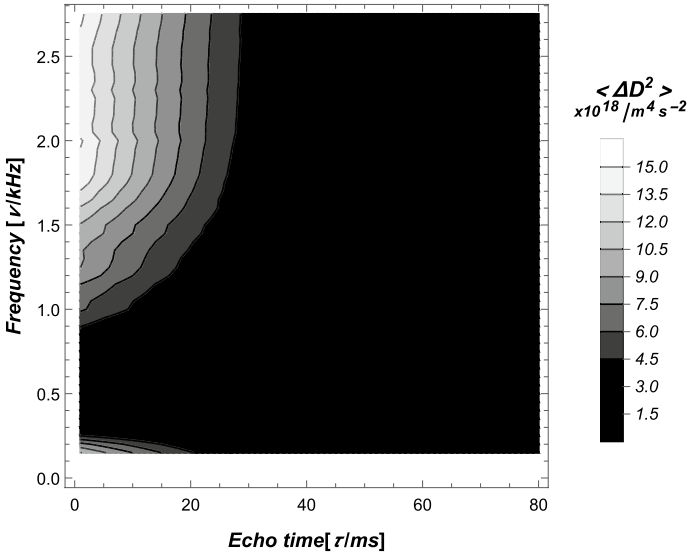

Fig. 2 The contour plot of the distribution variance of the diffusion coefficient, $\langle \Delta D^2 \rangle$, in water showing the diversity of molecular motion observed only at short observation times and at high modulation frequencies

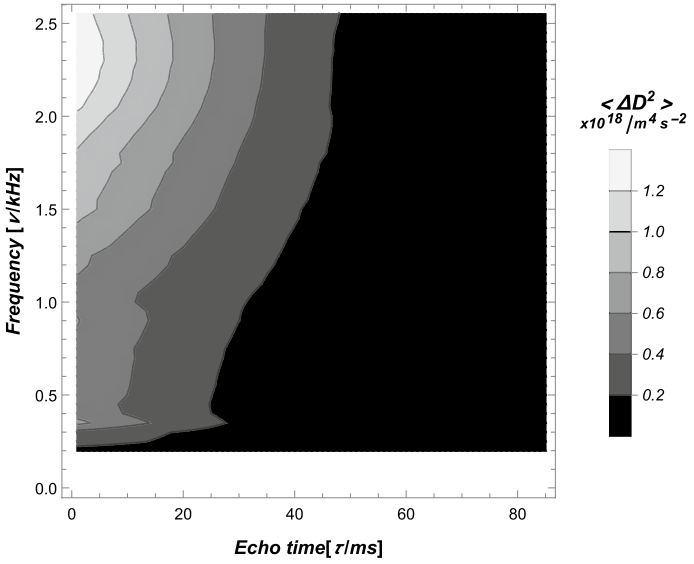

Fig. 3 The contour plot of $\langle \Delta D^2 \rangle$ in ethanol

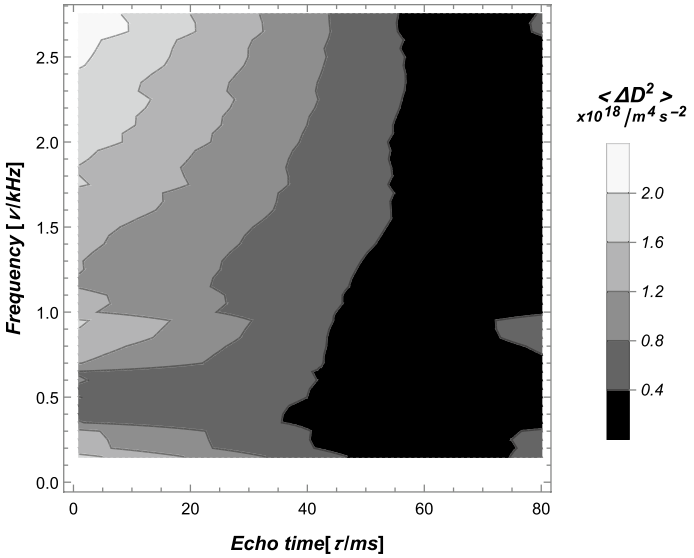

Fig. 4 The contour plot of $\langle \Delta D^2 \rangle$ in toluene

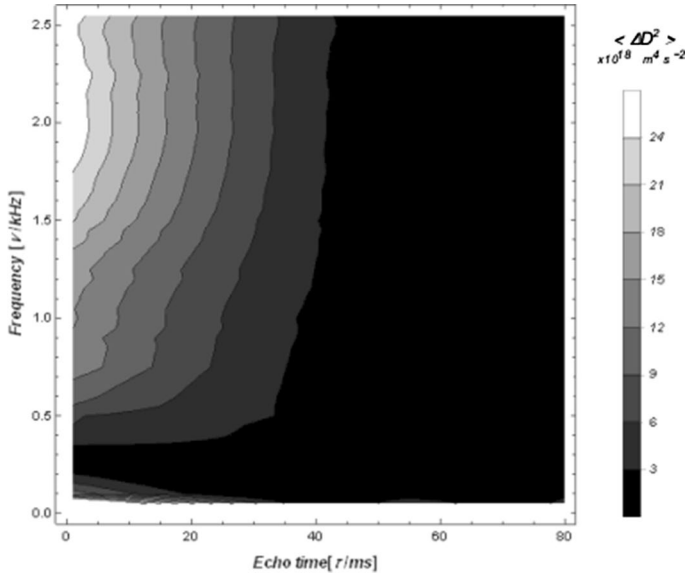

Fig. 5 The contour plot of $\langle \Delta D^2 \rangle$ in the G/W mixture with 5 vol% of glycerol

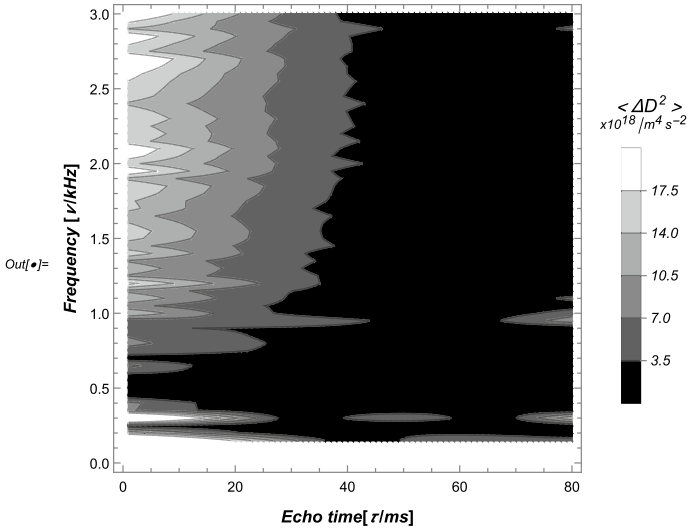

Fig. 6 The contour plot of $\langle \Delta D^2 \rangle$ in the G/W mixture with 15 vol% of glycerol demonstrating how fluctuations weaken with increasing glycerol content

Table 1 Parameters of hydrodynamic fluctuations

sample	$D/10^{-9}\,\mathrm{m^2 s^{-1}}$	τ_c/ms	$\Delta z/\mu\mathrm{m}$
Toluene	3.17	1.02	1.4
Ethanol	1.12	0.83	2.8
Water	2.19	0.71	4.2
G/W 5 vol%	2.73	0.90	5.7

5 Conclusion

In conclusion, we can state that the non-exponential decay of spin-echos in the initial short-time intervals of MGSE measurements of water, ethanol, toluene, and glycerol/water mixtures unambiguously confirms an existence of diversity of diffusion in bulk of liquids, which is not, for instance, the consequence of media inhomogeneity as observed in the diffusion measurement in the porous system, but appears due to diversity of motion in liquids. Given that the method provides the time average of VAS over the elapsed particle trajectories, we attribute them to the spatial diffusion heterogeneity caused by molecular motion in microvortices of hydrodynamic fluctuations. The VAS variance images, $\langle \Delta D^2 \rangle$, clearly show the diversity attributed to hydrodynamic fluctuation occurring in the high-frequency range of higher frequencies, which allows the estimation of the fluctuation correlation time, τ_c , and are also noticeable in the initial measurement times when spin trajectories are short, allowing the size of the hydrodynamic vortices to be estimated. At longer time intervals,

when the spin path crosses the entire space diversity, the inhomogeneity is averaged off and the image of diversity disappears.

The MGSE measurement of pure glycerol by NMR MOUSE [26] does not exhibit any dependence on echo times. We speculate that the vortexes of its hydrodynamic fluctuation are too fast and too narrow to be observed at the shortest time intervals T attainable by our device. This is also confirmed by the fact that the correlation times of molecular motion in pure glycerol are about ten times shorter than in water and ethanol, which corresponds to the magnitude of the dipole moments of these liquids [26].

Thus, we can conclude that the MGSE method displays an unusual diversity of the molecular self-diffusion in pure liquids and glycerol/water mixtures, which can be explained as a combination of molecular self-diffusion and eddy diffusion processes [12] in the vortexes of hydrodynamic fluctuations.

Acknowledgements We acknowledge the participation of A. Mohorič and Igor Serša from the University of Ljubljana, Slovenia, as well as Carlos Mattea from the Technical University, Ilmeanau, Germany, in the preparation of the experiments.

Funding Research was funded by the grant of the Slovenian research agency, ARRS, for the program P1-0060: "Experimental biophysics of complex systems and imaging in bio-medicine".

Compliance with Ethical Standards

Conflict of interest The author has no conflict of interest.

References

1. M. Aggarwal, M. Jones, P. Calabresi, S. Mori, J. Zhang, Magn. Reson. Med. **67**, 98–109 (2012). https://doi.org/10.1002/mrm.22981
2. B. Alder, T. Wainwright, Phys. Rev. Lett. **18**, 988–90 (1967)
3. B. Alder, T. Wainwright, Phys. Rev. A **1**, 18–21 (1970)
4. V. Ardente, G. Nardelli, L. Reatto, Phys. Rev. **148**, 124–138 (1966)
5. J.P. Boon, S. Yip, *Molecular Hydrodynamics* (Dover Publications Incorporated, New York, 2013)
6. F. Croccolo, J.M.O. de Zarate, J.V. Sengers, Eur. Phys. J. E **39**, 125 (2016)
7. P. Callaghan, J. Stepišnik, J. Magn. Reson. A **117**, 118–122 (1995)
8. P. Callaghan, J. Stepišnik, in *Generalised Analysis of Motion Using Magnetic Field Gradients*, vol. 19, ed. by S.W. Warren (Academic Press, Inc, San Diego, 1996), pp. 326–389
9. P.T. Callaghan, S.L. Codd, Phys. Fluids **13**, 421–6 (2001)
10. H.Y. Carr, E.M. Purcell, Phys. Rev. **94**, 630–38 (1954)
11. M.S. Giterman, M.E. Gertsenshtein, J. Exp. Theor. Phys. **23**, 723–728 (1966)
12. D.I. Graham, Int. J. Multiph. Flow **27**, 1065–1077 (2001)
13. L. Landau, E. Lifshitz, *Fluid Mechanics (Volume 6 of A Course of Theoretical Physics)* (Pergamon Press, Oxford, 1959)
14. L.D. Landau, E.M. Lifshitz, J. Exp. Theor. Phys. **32**, 618–619 (1957)
15. K.F. Larsson, Phys. Rev. **167**, 171–182 (1968)
16. S. Lasič, J. Stepišnik, A. Mohorič, I. Serša, G. Planinšič, Europhys. Lett. **75**, 887–93 (2006)
17. G. Maret, P. Wolf, Z. Phys. B **65**, 409–423 (1987)
18. S. Meiboom, D. Gill, Rev. Sci. Instrum. **29**, 688–91 (1958)
19. E.C. Parsons, M.D. Does, J.C. Gore, Magn. Reson. Imaging **21**, 279–85 (2003)
20. M. Sakamoto, J. Phys. Soc. Jpn. **19**, 1862–1866 (1964)

21. J. Stepišnik, Phys. B **104**, 350–64 (1981)
22. J. Stepišnik, Prog. Nucl. Magn. Reson. Spectrosc. **17**, 187–209 (1985)
23. J. Stepišnik, Europhys. Lett. **60**, 453–59 (2002)
24. J. Stepišnik, I. Ardelean, J. Magn. Reson. **272**, 100–107 (2016)
25. J. Stepišnik, P. Callaghan, Phys. B **292**, 296–301 (2000)
26. J. Stepišnik, C. Mattea, S. Stapf, A. Mohorič, Eur. Phys. J. B **91**, 293 (2018). https://doi.org/10.1140/epjb/e2018-90284-4
27. J. Stepišnik, C. Mattea, S. Stapf, A. Mohorič, Phys. Stat. Mech. Appl. (2020). https://doi.org/10.1016/j.physa.2020.124171
28. J. Stepišnik, A. Mohorič, C. Mattea, S. Stapf, I. Serša, Europhys. Lett. **106**, 27007 (2014)
29. D. Topgaard, C. Malmborg, O. Soederman, J. Magn. Reson. **156**, 195–201 (2002)
30. V. Vladimirsky, J. Terletzky, J. Exp. Theor. Phys. **15**, 258–263 (1945)